Optimal Resource Placement for Electric Grid Resilience via Network Topology

Balasubramanian Sambasivam[1*], **Connor Colombe**[1], **John Hasenbein**[1], **Benjamin Leibowicz**[1]

[1] Operations Research and Industrial Engineering, University of Texas at Austin, 204 E Dean Keeton St, Austin, TX 78712, USA

Abstract

In this paper, we investigate the resilience of alternative electric grid configurations by adopting a stylized approach based on graph theory, probabilistic analysis, and simulation. We consider two alternative classes of electricity network topology: binary trees and rectangular lattices. For each topology, we derive the probabilities that customers located at various nodes in the network will continue to have power following a disaster, depending on the locations of resources (e.g., generators, storage units) in the network. Then, these probabilities are incorporated into the problem of optimally placing resources throughout the network. This is a cost-benefit problem that weighs the benefits of placing resources closer to customers – that is, pursuing a distributed resilience strategy – against the higher total cost of deploying a greater number of smaller resource units. Our analytical and numerical results thus shed light on the general circumstances in which centralized or distributed resilience strategies are preferable. While optimal resource placements depend on various assumptions, such as the probability that power lines fail and the strength of economies of scale, we find that distributed resilience strategies are more often preferred in the binary tree topology than in the rectangular lattice topology. Rectangular lattices feature greater redundancy in terms of paths between nodes in the network, enabling the system to be fairly resilient even with centralized resources.

KEY WORDS: resilience, electricity, networks, probability, simulation, cost-benefit analysis

[*]**Corresponding author.** *E-mail address: balasubramaniansa@austin.utexas.edu*

1. Introduction

Ensuring the reliable provision of electricity is essential for the smooth operation of critical infrastructure sectors such as healthcare, water, defense, and communications (Mishra and Anderson, 2021) and more generally to ensure economic stability and security. Extreme weather events such as hurricanes, snow and ice storms, and heavy thunderstorms pose significant threats to electric transmission and distribution networks and have been responsible for major outages in the recent past. Therefore, increasing the resilience of the electricity network to withstand such extreme events is imperative. In recent years there have been significant disruptions to the electricity networks associated with Superstorm Sandy and Hurricanes Harvey, Irma, and Maria (Wender et al., 2017; Poudel et al., 2019; Sharma and Chen, 2020; Watson and Etemadi, 2020). In 2017 in Texas, due to Hurricane Harvey, the total number of electric customer outages stood at 2 million, and it took almost two weeks to completely restore power to all customers. In 2017 and 2018, the total damages due to these extreme events were about \$3.3 and \$3.0 billion, respectively (Chen et al., 2019). The latest in this line of natural disasters was Winter Storm Uri, which caused substantial economic losses of about \$130 billion in Texas in February 2021 (Busby et al., 2021). In the aftermath of Uri, more than 4 million people were left without electricity for almost a week, and among the 69% of Texans who experienced an outage, the average outage duration was 42 hours (Kemabonta, 2021). The total annual cost of power interruptions in the U.S. is about \$44 billion (LaCommare et al., 2018). This situation has led to an increased focus on the resilience of the electric grid.

Resilience refers to the ability of the electricity system to recover quickly after a major disaster and adapt its structure and operational procedures to mitigate the impact of future extreme events. Presidential Policy Directive (PPD) 21 defines grid resilience as "the ability to prepare and plan for, absorb, recover from, or more successfully adapt to actual or potential adverse events (Alderson et al., 2015; Bessani et al., 2019)." Resilience can be divided into two categories: operational and infrastructure resilience (Panteli and Mancarella, 2015). Operational resilience relates to the loss of load and expected demand not being met in the event of a grid outage due to an extreme event. Infrastructure resilience relates to the damages to electric infrastructure caused by the extreme event. Reliability and resilience are two important electricity system properties that describe the ability of the system to satisfy demand. In general, reliability guards against high-probability, low-impact events such as electric system faults, while resilience guards against low-probability, high-impact events (i.e., extreme events) such as hurricanes, snow storms, and so on. These extreme events have the potential to disrupt electricity service on large spatial and temporal scales, with severe consequences extending from financial losses to losses of lives. So, designing electricity systems to be resilient against extreme weather threats is a critical objective of planners and a topic of great interest to researchers.

Publications on critical infrastructure and network resilience have increased significantly over the last few years, which can be attributed to the increasing frequency of natural disasters (Curt and Tacnet, 2018). This literature has empirically studied the impacts of historical extreme weather events on the power sector. Other contributions use optimization to analyze how to design and operate electricity systems to achieve greater resilience. However, a common limitation of these studies is that they rely on computational models that are highly data-intensive and produce results that are difficult to generalize, as they are specific to one particular case study parameterization. To address this issue, we analyze stylized models to provide broader insights into resilience enhancement strategies.

Our objective is to investigate the resilience of alternative electric grid configurations by adopting a stylized approach based on graph theory, probabilistic analysis, and simulation. We consider two alternative classes of electricity network topology: binary trees and rectangular lattices. We choose these two topologies because they resemble real-world electric grids and represent opposite extremes in terms of network redundancy. A binary tree has no redundancy since there is only one path from the root node to each leaf. In contrast, the rectangular lattice has much greater redundancy, as there are multiple paths between any two nodes. For each topology, we derive the probability that a customer located at various nodes in the network will continue to have power following a disaster, depending on the locations of resources (e.g., generators, storage units) in the network. Then, these probabilities are incorporated into the problem of optimally placing resources throughout the network. This is a cost-benefit problem that weighs the benefits of placing resources closer to customers – that is, pursuing a distributed resilience strategy – against the higher total cost of deploying a greater number of smaller resource units. Our analytical and numerical results thus shed light on the general circumstances in which centralized or distributed resilience strategies are preferable. While optimal resource placements depend on various assumptions, such as the probability that power lines fail and the strength of economies of scale, we find that distributed resilience strategies are more often preferred in the binary tree topology than in the rectangular lattice topology. Rectangular lattices feature greater redundancy in terms of paths between nodes in the network, enabling the system to be fairly resilient even with centralized resources.

The remainder of this paper is organized as follows. In Section 2, we provide a detailed review of the most relevant literature. Our analysis of the binary tree in Section 3 combines several theoretical results with numerical examples. Section 4 describes our numerical analysis of the rectangular lattice, which employs simulation to compute probabilities. In Section 5, we compare optimal resource placements in the binary tree and rectangular lattice topologies. Section 6 concludes by summarizing our most significant contributions and identifying directions for future research.

2. Literature review

The most relevant literature on electricity resilience can be divided into data-intensive computational models with a specific case study focus, and conceptual studies which discuss high-level ideas and policies for improving resilience.

2.1. Computational models for electric grid resilience

Optimization models are widely employed to study decision-making for enhancing grid resilience. Gharehveran et al. (2022) proposed a two-stage mixed-integer quadratic programming model for a microgrid framework with solar panels, micro-turbines, and mobile batteries to make an electricity system more resilient against extreme events. Investment decisions are considered in the first stage, and in the second stage, operational variables are chosen to improve the resilience of the system. Ashrafi et al. (2021) proposed a multi-objective optimization approach based on a genetic algorithm and an epsilon constraint method to enhance grid resilience in a smart grid environment with distributed energy storage during extreme weather conditions. The study's objectives include minimizing the distribution network operational cost and the penalty cost for energy not supplied, and maximizing benefits for the energy suppliers. Zhang et al. (2021) used a combinatorial network configuration and double-loop optimization methodology to derive quick recovery methods for post-disaster networks, supplying the largest amount of electricity on a fixed topology (IEEE 188-Bus System). Here, the objective is to effectively reorganize the system to supply power to a topology with the largest demand requirement. Hardening the electric grid is considered essential for improving resilience. Ma et al. (2016) presented a tri-level optimization problem to minimize load shedding by making electric grid hardening investments to enhance distribution system resilience during extreme events. Ma et al. (2018) proposed a two-stage stochastic mixed-integer programming problem to develop a resilience-oriented design technique for enhancing the distribution grid's resilience during extreme events. The problem focuses on hardening the distribution lines, deploying distributed generators, and reducing system operation and repair costs. Alderson et al. (2015) proposed operational models to assess infrastructure system operational resilience, identify critical vulnerabilities, and advise policymakers on appropriate investments for improving resilience.

Electricity supply interruptions can severely impact operations at critical facilities and businesses such as airports, hospitals, offices, and hotels. So, developing models to explore potential resilience strategies for these facilities is crucial. Masrur et al. (2021) proposed a mixed-integer linear programming (MILP) model for the techno-economic assessment of grid-connected microgrids with renewable energy sources, batteries, and diesel generators to improve grid resilience. As a case study, the model is applied to study Logan

International Airport in Boston, Massachusetts. Liu et al. (2021) proposed an optimization model to improve the resilience of hospitals during unpredicted electricity outages with a hybrid microgrid consisting of wind turbines, diesel generators, and energy storage units. The outages are generated randomly over different days of the year, and a resilience index is computed based on the unmet electricity demand. Sepúlveda-Mora and Hegedus (2022) proposed a hybrid microgrid with solar photovoltaics (PV), wind, and battery storage to increase the resilience of commercial buildings in three locations with different consumption types using the Homer Grid software. The study considers three locations: Tucson, Arizona; Sioux Falls, South Dakota; and Wilmington, Delaware. The results show that the proposed hybrid microgrid could withstand a three-day power outage in all three locations. Laws et al. (2018) performed a techno-economic assessment of the value of resilience achieved via solar PV and battery storage using an MILP model. The model is tested on a large hotel in Anaheim, California. Ishiwata and Yokomatsu (2018) formulated a dynamic stochastic macroeconomic model to quantitatively examine the economic impacts of disasters on developing countries, using Pakistan as the case study.

Setting up a microgrid with different generation options is viewed as an effective strategy for enhancing grid resilience. So, identifying ideal locations for developing microgrids is imperative for managing technical and economic constraints. Related to our study of optimal resource placement, Aros-Vera et al. (2021) proposed a facility location model to evaluate the potential of microgrids to increase the resilience of critical infrastructure (CI) networks. The model's objective is to find the ideal locations for microgrid installation by minimizing the weighted distance of population centers to the CI while considering system capacity. To improve resilience during a large-scale grid disturbance, Kizito et al. (2020) formulated a facility location coverage problem to optimize the number of renewable distributed generators in a utility-based microgrid, considering budgetary constraints. The model's objective is to minimize the operation and maintenance costs, investment costs, and the distance traveled for electricity distribution.

Many researchers have developed metrics for measuring an electricity system's resilience. In extreme weather conditions, to analyze the resilience of electric grids with integrated microgrids, Liu et al. (2016) proposed four different resilience indices: loss of load probability, line outage, expected demand not met, and difficulty level of grid recovery. They use a mesh grid approach to model the extreme events and a Markov chain to analyze the electric grid's state transitions. The resilience indices are calculated using Monte Carlo simulation. To quantify the operational resilience of an electric grid, Poudel et al. (2019) proposed a probabilistic metric based on Conditional Value-at-Risk (CVaR). The proposed metric is evaluated using a simulation approach on an IEEE 123-bus test system. With many metrics developed to measure system resilience, testing the validity of the metrics is critical. To test the validity of resilience metrics against its conceptual framework, Najarian and Lim (2019) proposed a methodology based on experimental design methods and statistical analysis techniques.

Researchers have developed different approaches to evaluate the resilience of transmission and distribution networks. Galvan et al. (2020) assessed the resilience of the distribution grid to natural disasters with networked microgrids and distributed energy resources based on the Resilience Analysis Process (RAP). In this study, resilience analysis focuses on low-probability, high-consequence events, and the metrics focus on the event's impact on humans. Trakas et al. (2019) developed a severity risk index based on probabilistic risk by considering system operating conditions, degraded system performance, and spatial and temporal evolution of the extreme event to assess its impact on the resilience of electric transmission networks. Gallaher et al. (2021) employed spatial econometrics to investigate the impact of tree trimming operations on improving electric grid resilience in Connecticut, using an outage events dataset from 2009 to 2015 from New England's largest utility company, Eversource Energy.

As described above, the literature includes many examples of optimization models designed to determine grid resilience enhancement strategies. These optimization models are highly data-intensive and produce results that are specific to one case study parameterization. In contrast, our study leverages stylized models, theoretical analysis, and simulation in order to obtain more general insights into grid resilience decision-making. Our study is related to Kizito et al. (2020) and Aros-Vera et al. (2021) in that we focus on decisions about where to place resources within electricity networks.

2.2. Conceptual studies on electric grid resilience

Expert perspectives impart new knowledge and play a vital role in guiding strategies for resilience enhancement. Brown and Soni (2019) studied the concept of improving electric grid resilience with electric vehicle integration using the Delphi approach. Experts from the U.S. Department of Energy's Electricity Advisory Committee were surveyed, and the results were compared to the existing literature, policy paradigms, and the concerned stakeholders. Chang et al. (2014) proposed an approach based on expert judgments to characterize a community's infrastructure vulnerability and resilience against disasters. They test their proposed framework on a case study of earthquake and flood risks in metro Vancouver, Canada. Due to the increasing frequency of natural disasters and associated grid disturbances in the U.S., the federal government has introduced several programs for community investments to improve electricity resilience. Zamuda and Ressler (2020) highlight the list of federal programs and funding opportunities available to enhance electricity resilience during extreme weather conditions.

Since improving electricity resilience involves different stakeholders, appropriately weighing each criterion for decision-making deserves specific attention. Based on three resilience dimensions – "resist," "restabilize," and “recover” – Siskos and Burgherr (2022) proposed a multicriteria decision support framework to evaluate the electricity supply resilience of 35 European countries using their performance on 17 evaluation criteria. The evaluation criteria are based on electricity generation mix, supply, availability and outage, and the country's political and economic stability. The crisis management cycle can be conceptualized as having four phases: preparedness, response, recovery, and mitigation. Understanding the different phases in the crisis management cycle and preparing suitable methods for addressing each phase requires significant attention. Forssén and Mäki (2016) present different conceptual methods to address grid resilience during an extreme event based on the four phases of the crisis management cycle for the Finnish electricity system. In conceptual studies, the expert opinions are based on a specific set of evaluation criteria considering the different phases in the extreme event scenario.

From our point of view, there is a lack of theoretical work on electric grid resilience that is capable of yielding broad, generalizable insights into resilience decision-making. In this study, we develop stylized models of electricity resilience in grids with two types of regular network topology: binary trees and rectangular lattices. We study the problem of optimally placing resources in these electric grids, considering both the costs and benefits of pursuing a distributed resilience strategy with a greater number of smaller resource units located closer to customers. The sections that follow include a combination of theoretical and numerical analysis.

3. Resilience analysis for a binary tree topology

Each of our analyses begins with a regular electric grid topology (e.g., binary tree, rectangular lattice) and assumptions about the failure probabilities of infrastructure components (e.g., the probability that any one line is destroyed). We consider different placements of resources, such as power plants or batteries, throughout the network. For the binary tree, we derive the probabilities that customers located at various nodes in the network continue to have power following a disaster, depending on the locations of resources (e.g., generators, storage units) in the network. Then, these probabilities are incorporated into the problem of optimally placing resources throughout the network. This is a cost-benefit problem that weighs the benefits of placing resources closer to customers — that is, pursuing a distributed resilience strategy — against the higher total cost of deploying a greater number of smaller resource units.

We now outline our approach for the binary tree topology. Suppose we have a perfect binary tree T of height $h \geq 0$ (where $h = 0$ represents a single-node binary tree) as represented in Figure 1a. In Figure 1a, R and C denote the resource and customer nodes, respectively. In our model we will always assume that the customer nodes are the leaves of the binary tree. Furthermore, we assume that power always flows from a resource node to a customer node along the most direct route (i.e., along the unique shortest path from

R to C). In addition, suppose that the probability that any given edge in the tree succeeds in transferring power is p and the probability that the edge fails to transfer power (e.g., due to extreme weather or some other adverse event) is $1-p$. We assume that the edge failures are mutually independent. Given this setup, we face the problem of identifying the layer $g \in \{0, 1, 2, \ldots, h\}$ at which to place resources to provide power to the customers located at the leaf nodes. To place resources at layer g in T means to establish each of the 2^g leaves of the rooted height g sub-tree of T as a resource node. Since power may only flow downstream from the resource nodes to the customer nodes, this creates 2^g identical sub-trees of height $h-g$, each with a resource at its root node and 2^{h-g} customers at its leaf nodes. Examples of such scenarios are depicted in Figure 1. We also assume that customers all have the same constant power demand, and therefore the total resource capacity is the same regardless of the resource placement g.

3.1. Expected number of customers with power in a binary tree

For a given binary tree network with parameters h, g, and p, we now compute the expected number of customers (i.e., leaf nodes) with power. Fortunately, we can exploit the symmetric and recursive nature of our problem along with the linearity of expectation.

Theorem 1. *Consider a perfect binary tree of height h, and suppose we place 2^g resources in layer $g \leq h$. Let p be the probability that power is transferred along any given edge, and assume that edge failures are mutually independent. Then, the expected number of customers with power is given by $2^h p^{h-g}$.*

Proof. To begin, note that there are 2^g independent sub-trees of height $h-g$. Let the number of leaves with power in each sub-tree be denoted $N_1, N_2, \ldots, N_{2^g}$, respectively. Then, the expected number of leaves with power in the entire tree is given by

$$\mathbb{E}\left[N_1 + N_2 + \ldots + N_{2^g}\right] = 2^g \, \mathbb{E}[N_1],$$

where we used the fact that the N_i are identically distributed. Now consider one of these single resource sub-trees. It has height $h-g$ and thus 2^{h-g} leaves. Let $X_1, X_2, \ldots, X_{2^{h-g}}$ be i.i.d. indicator variables, with each indicating whether the corresponding leaf has power. Then, we can write

$$\mathbb{E}[N_1] = \mathbb{E}\left[X_1 + X_2 + \ldots + X_{2^{h-g}}\right] = 2^{h-g}\mathbb{E}[X_1] = 2^{h-g}\mathbb{P}[X_1 = 1].$$

For the penultimate step, we need to evaluate $\mathbb{P}[X_1 = 1]$. In a single resource sub-tree, the only way a particular leaf gets power is if each of the lines on the unique path between it and the root succeeds in transferring power. In our case, this implies that $\mathbb{P}[X_1 = 1] = p^{h-g}$.

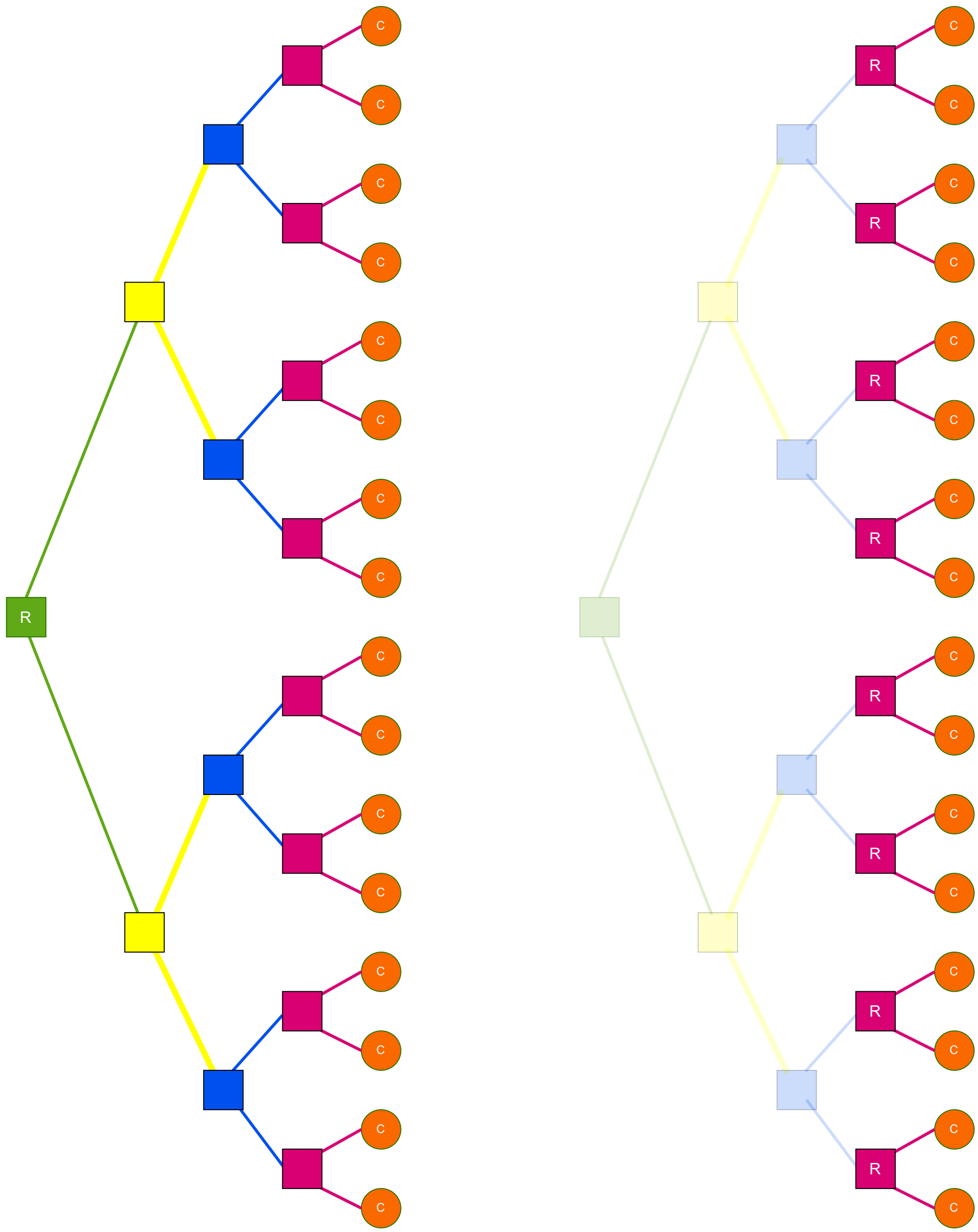

(a) Binary tree of height $h = 4$ with resource placement at $g = 0$.

(b) The configuration with resources at $g = 3$ can be interpreted as eight small, identical sub-trees.

Figure 1. Binary tree topology

Thus, $\mathbb{E}[N_1] = (2p)^{h-g}$ and

$$
\begin{aligned}
\mathbb{E}\left[N_1 + N_2 + \ldots + N_{2^g}\right] &= 2^g \, \mathbb{E}[N_1] \\
&= 2^g (2p)^{h-g} \\
&= 2^h \, p^{h-g},
\end{aligned}
$$

as desired. $\square$

3.2. Optimal resource placement in a binary tree

Having derived an exact expression for the expected number of leaves with power in a perfect binary tree network of height h and rooted perfect resource sub-tree of depth g, the next step is to find the optimal resource placement in the tree. For the purposes of this paper, we model a decision-maker whose alternatives are the different layers in the network in which resources can be placed. Their goal is to identify layer $g^* \in \{0, 1, \ldots, h\}$ such that the expected net benefit is maximized. To motivate why different placements matter, consider placing a single resource at layer $g = 0$. For any $0 < p < 1$, the expected number of customer nodes with power is minimized, but we only have to install a single (large) resource. On the other hand, placing resources at $g = h$ ensures that every customer node will have power but the planner must install 2^h (smaller) resources, which may be very costly. Fundamentally, we are interested in finding the ideal balance between placing resources closer to customers, which improves resilience, and placing (fewer but larger) resources closer to the root node, which is less costly due to economies of scale. We now begin to formulate our model.

Let B be the benefit in dollars of a single customer receiving power. We introduce the random variable N_g that represents the number of customers with power given a choice to install the resources at layer g. The cost of placing resources in a given layer can be broken down as follows:

$$\begin{aligned} Cost &= (\#\text{ of resources placed}) \times (\text{power capacity of each resource}) \times \\ &\quad (\text{cost per unit of power at the given capacity}) \\ &= n \times \left(\frac{d}{n}\right) \times \ell\left(\frac{d}{n}\right) \\ &= d \times \ell\left(\frac{d}{n}\right), \end{aligned}$$

where n is the number of resources placed, d is the total power demand, and $\ell(x)$ is a function denoting the cost per unit power capacity for a resource with power capacity x. In order to account for economies of scale, $\ell(x)$ should be decreasing in x, as this implies that larger resources are cheaper to deploy on a per-unit-capacity basis. We use the function $\ell(x) = Ax^{-m} + C$ where C is the cost per unit of power for an infinitely large resource, A is a scaling parameter, and $m > 0$ reflects the strength of economies of scale. More precisely, as m increases, the cost per unit of power decreases for a given capacity. If we take the mixed partial derivative of $\ell(\cdot)$ with respect to capacity x and then our economies of scale parameter m, we find

$$\frac{\partial^2 \ell}{\partial x \partial m} = Ax^{-(m+1)} \left(m \log(x) - 1\right),$$

which is strictly negative for $0 < x \leq e^{1/m}$. To ensure that a higher value of m can be straightforwardly interpreted as signifying stronger economies of scale, we restrict the capacity x to the interval [0,1].

In our numerical analyses we will only consider values of $m \in (0, 1]$; over this interval, larger values of m correspond to stronger economies of scale. In the case of our binary tree topology, we have $n = 2^g$, $d = 1$ (we assume that each customer has an identical fraction of the total unit demand), and therefore the capacity of each resource in layer g is 2^{-g}. Altogether, the total cost of placing resources in layer g is $\Big(A\,(2^{-g})^{-m} + C\Big)$. The notation for our optimization model is listed in **Table 1**. The general form of the optimization problem is therefore:

Table 1. Notation for the binary tree analysis

Sets and Indices	
h	The height of the binary tree network
2^h	Total number of customers (i.e., leaf nodes) in the network
Variables	
g	Layer at which resources are placed
N_g	The random variable denoting the number of customers with power given resources in layer g
n	Number of resources placed
Parameters	
B	Monetary benefit per customer receiving power
A	Cost function scaling parameter
C	Theoretical lower bound on resource cost per unit capacity
m	A positive scaling parameter that controls the strength of economies of scale
d	Total power demand

$$\begin{aligned}\max_{g\in\{0,1\ldots,h\}} \mathbb{E}[(\text{Benefit})_g - (\text{Cost})_g] &= \max_{g\in\{0,1\ldots,h\}} B\,\mathbb{E}\left[N_g\right] - \Big(A\left(2^{-g}\right)^{-m} + C\Big)\\ &= \max_{g\in\{0,1\ldots,h\}} B\,2^h p^{h-g} - (A2^{gm} + C)\\ &= -C + 2^h \max_{g\in\{0,1\ldots,h\}} Bp^{h-g} - A2^{gm-h}.\end{aligned}$$

Based on the above, if we want to solve for the optimal resource placement layer g^*, it suffices to solve the optimization problem

$$\max_{g\in\{0,1\ldots,h\}} Bp^{h-g} - A2^{gm-h}. \tag{1}$$

3.3. Analytical solution for optimal resource placement in a binary tree

Determining the optimal resource layer in (1) involves solving over the set of integers $\{0, \ldots, h\}$. We begin by initially solving (1) using the continuous relaxation of the problem,

$$\max_{g \in [0,h]} f(g) = Bp^{h-g} - A2^{gm-h}, \tag{2}$$

and then use this to obtain the optimal integer solution. Before deriving the optimal solution to the continuous optimization problem (2), we need the following lemma.

Lemma 1. *The function $f(g) = Bp^{h-g} - A2^{gm-h}$ has a unique critical point on $\mathbb{R}$ if $2^m p \neq 1$. Furthermore, this critical point is a unique global maximum if and only if $2^m p > 1$ and a unique global minimum if and only if $2^m p < 1$.*

Proof. The critical points of f are the solutions to the equation $f'(g) = 0$, which can also be expressed as

$$\frac{B(2p)^h \log\left(\frac{1}{p}\right)}{A \log 2^m} = (2^m p)^g. \tag{3}$$

If $2^m p \neq 1$, then the right-hand side of (3) is a strictly monotonic continuous function of g with domain $\mathbb{R}$ and range $\mathbb{R}_+$ and the left-hand side is a positive constant. It follows that there exists a unique solution g^* and thus a unique critical point.

Solving for g^*, we obtain

$$g^* = \frac{\log\left(\frac{B(2p)^h \log\left(\frac{1}{p}\right)}{A \log 2^m}\right)}{\log 2^m p}. \tag{4}$$

Next, we show that g^* is a unique global maximum if $f''(g^*) < 0$. The proof that g^* is a unique global minimum when $f''(g^*) > 0$ is analogous. Suppose $f''(g^*) < 0$ and g^* is not a unique global maximum. Then there must exist some $g' \in \mathbb{R}$ such that $f(g^*) \leq f(g')$. WLOG let $g' > g^*$. We will now use Taylor's Theorem to argue that $f(g^* + \epsilon) < f(g^*)$ for sufficiently small $\epsilon > 0$. By Taylor's Theorem, since $f(g)$ is a twice-continuously differentiable function, we have that

$$f(g^* + \epsilon) = f(g^*) + \epsilon f'(g^*) + \frac{\epsilon^2}{2} f''(g^* + t\epsilon) \tag{5}$$

for some $t \in (0,1)$. Noting that $f'(g^*) = 0$, we can rearrange (5) to obtain

$$f(g^* + \epsilon) - f(g^*) = \frac{\epsilon^2}{2} f''(g^* + \alpha) \tag{6}$$

for some $\alpha \in (0, \epsilon)$. Now, since $f''(g)$ is a continuous function and $f''(g^*) < 0$, we can let ϵ be sufficiently small such that the right-hand side of (6) is negative, implying that $f(g)$ decreases in a sufficiently small neighborhood of g^*.

Therefore, since f is a continuous function, it follows that there must be some $\overline{g} \in (g^*, g')$ such that $f(g^*) = f(\overline{g})$ by the intermediate value theorem. But Rolle's theorem then implies that there is a point $\hat{g}$ on the interval $(g^*, \overline{g})$ at which $f'(\hat{g}) = 0$, contradicting the fact that g^* is the unique critical point of f. Therefore, there does not exist a g' such that $f(g') \geq f(g^*)$, implying that g^* is the unique global maximizer of $f(g)$, as desired.

Lastly, we need to show that $f''(g^*) < 0$ if and only if $2^m p > 1$ (the proof of $f''(g^*) > 0$ if and only if $2^m p < 1$ follows the same logic). Setting $f''(g^*) < 0$ and rearranging terms, we get the inequality

$$\frac{B(2p)^h \log(p)^2}{A \log(2^m)^2} < (2^m p)^{g^*}.$$

Taking the logarithm of both sides and plugging in (4) for g^* yields the inequality

$$\log\left(\frac{B(2p)^h \log(p)^2}{A \log(2^m)^2}\right) < \log\left(\frac{B(2p)^h \log\left(\frac{1}{p}\right)}{A \log 2^m}\right).$$

Since the logarithm is a strictly increasing function we can drop the logarithms and cancel positive like terms to obtain

$$\frac{\log(p)^2}{\log(2^m)^2} < \frac{\log\left(\frac{1}{p}\right)}{\log 2^m}.$$

One last round of rearrangement and cancellation of positive terms gives the condition $0 < \log(2^m p)$, which is true if and only if $2^m p > 1$. As all of the logical steps above are reversible, we conclude that $f''(g^*) < 0$ if and only if $2^m p > 1$. Analogous arguments yield that $f''(g^*) > 0$ if and only if $2^m p < 1$, completing the proof. $\square$

Before moving on to our main results, we examine how our expression for g^* is affected by our choice of parameters. We can easily see from (4) that increasing the value of B, the monetary benefit of a single customer receiving power, causes g^* to increase. That is, as the benefit of each customer receiving power increases, the optimal resource placement layer is closer to the customers, in order to increase the expected number of customers with power. On the other hand, if we increase A, which reflects the cost per unit of resource capacity, we see that g^* will decrease. The intuitive explanation is that as the cost of investing in resources increases, placing more resources becomes more costly and thus it is advantageous to place resources more centrally.

If we take the partial derivative of g^* with respect to h, we find that $\frac{\partial g^*}{\partial h} = \frac{\log 2p}{\log(2^m p)}$, which can be positive or negative depending on the values of p and m. In our case, if we assume that g^* is feasible and a global maximum ($g^* \in [0, h]$ and $2^m p > 1$), then $\frac{\partial g^*}{\partial h} > 0$ if and only if $p > 1/2$ while $\frac{\partial g^*}{\partial h} < 0$ if and only if $p < 1/2$. This implies that in a sufficiently reliable network with optimal resource layer $g^* \in (0, h)$, increasing the size of the network will cause the optimal resource layer to increase (i.e., move further away from the root node).

What is more interesting is examining the effects of p and m on g^*. Let us first look at the effects of p on g^*. Intuitively, we would expect that as p increases, signifying a more reliable network, the optimal resource placement layer would decrease. However, we find that the optimal resource layer can increase or decrease with p depending on the parameter values. If we again assume that g^* is feasible and a global maximum, then $\frac{\partial g^*}{\partial p}$ is negative if and only if $(h - g^*) \log \frac{1}{p} < 1$. Based on this, we can see that once a network is sufficiently reliable, increasing its reliability causes the optimal resource layer to shift towards the root, which is in line with our intuition. However, for networks where p is sufficiently small, this condition will not hold and increasing p will actually cause the optimal resource layer to move outward toward the customers.

Lastly, we examine the relationship between g^* and m, the economies of scale parameter. Intuitively, we would expect that as economies of scale get stronger we would see g^* decrease, and indeed that is what we see here. If we once more assume that g^* is feasible and optimal, then we obtain $\frac{\partial g^*}{\partial m} = \frac{-(1+g^* \log 2^m)}{m \log(2^m p)} < 0$, which implies that as economies of scale get stronger, the optimal resource layer should move inward toward the root node (i.e., become more centralized).

With Lemma 1 and the observations about g^* established, we may now state the main results regarding our continuous optimization problem.

Theorem 2. *Let* $g^* = \dfrac{\log\left(\frac{B(2p)^h \log\left(\frac{1}{p}\right)}{A \log 2^m}\right)}{\log 2^m p}$.

1. *If* $2^m p > 1$ *and* $0 \leq g^* \leq h$*, then* g^* *is the solution to the continuous optimization problem (2).*

2. *If* $2^m p \leq 1$ *or* $g^* \notin [0, h]$*, then the solution to the continuous optimization problem is* $g = 0$ *or* $g = h$*. In particular, the solution is* $g = 0$ *if*

$$p \geq \left(\frac{B - A2^{-h}\left(1 - 2^{hm}\right)}{B}\right)^{1/h} \tag{7}$$

and $g = h$ *otherwise.*

Proof. The first claim follows directly from Lemma 1 since g^* is a feasible solution to problem (2) and thus also the unique maximum on $[0, h]$.

To prove the second statement, we first show that if $2^m p \leq 1$, then the optimal solutions to the continuous optimization problem are at $g = 0$ or $g = h$. We have two cases to consider. If $2^m p = 1$, then the RHS of (3) is a constant in g and $f'(g) = 0$ has either zero or infinitely many solutions. If it has zero solutions, then $f(g)$ is a strictly monotonic function and the optimal resource placement must occur at $g = 0$ or $g = h$. On the other hand, if $f'(g) = 0$ has infinitely many solutions, then $f(g)$ is a constant function and thus $g = 0$ and $g = h$ are optimal resource placements.

In the second case, if $2^m p < 1$, then by Lemma 1, g^* exists and is a global minimum. The candidates for the maximum of $f(g)$ on $[0, h]$ are the set of critical points and the endpoints of the interval. Since g^* is the unique critical point and global minimum, the only candidates for the maximum on $[0, h]$ are $g = 0$ and $g = h$.

Next, suppose that $2^m p > 1$ but $g^* \notin [0, h]$. Since the potential candidates for maxima are the endpoints and critical points on the interval, and the interval does not contain the unique critical point, then the only candidates for maxima on $[0, h]$ are $g = 0$ and $g = h$.

Lastly, given that the optimal resource placement is one of the two endpoints, if we take the objective function in (2), evaluate it at $g = 0$ and $g = h$, set the $g = 0$ expression greater than or equal to the $g = h$ expression, and then isolate p, we arrive at (7). $\square$

With this result for the continuous optimization problem established, we note that the solutions to the continuous optimization problem (2) are not necessarily solutions to the original discrete optimization problem (1). Fortunately, the continuous optimization problem helps us easily identify solutions restricted to the integers.

Theorem 3. *Let* $g^* = \dfrac{\log\left(\frac{B(2p)^h \log\left(\frac{1}{p}\right)}{A \log 2^m}\right)}{\log 2^m p}$.

1. *If* $2^m p > 1$ *and* $0 \leq g^* \leq h$, *then any* $g \in \operatorname{argmax}\{f(\lfloor g^* \rfloor), f(\lceil g^* \rceil)\}$ *is an optimal solution to the discrete optimization problem (1).*

2. *If* $2^m p \leq 1$ *or* $g^* \notin [0, h]$, *then the optimal solution to the discrete optimization problem (1) is either* $g = 0$ *or* $g = h$. *The solution is* $g = 0$ *if*

$$p \geq \left(\frac{B - A2^{-h}\left(1 - 2^{hm}\right)}{B}\right)^{1/h}$$

   and $g = h$ *otherwise.*

Proof. 1. Suppose that $2^m p > 1$ and $g^* \in [0, h]$. If g^* is integer-valued then we are done. Otherwise, since g^* is the unique global maximum of $f(g)$ and unique critical point, $f(g)$ is strictly monotonically decreasing on either side of g^*. This implies that $\lfloor g^* \rfloor$ and $\lceil g^* \rceil$ are the only candidates for an optimal integer solution, and we simply choose the one that produces the larger objective value.

2. This follows immediately from case 2 of Theorem 2 since the two possible optimal resource placements are already integer-valued.

$\square$

3.4. Numerical analysis of a binary tree

To illustrate optimal resource placements in binary trees, we perform a numerical analysis of two different scenarios. The first scenario features weaker economies of scale (WEOS) in resource investment (specifically, we set $m = 0.1$), while the second scenario features stronger economies of scale (SEOS) ($m = 1$). All other model parameters are assigned the same values in both scenarios. We assume that the binary tree height is $h = 5$, the monetary benefit per customer receiving power is $B = 25$, the scaling parameter is $A = 20$, and the theoretical lower bound on cost per unit resource capacity is $C = 2$.

Figure 2 and **Figure 3** show the expected net benefit (i.e., the objective function) as a function of the resource placement layer – depicted as a continuous function – for scenarios with weaker and stronger economies of scale, respectively. The sub-figures within each figure represent different settings for p, the probability that an edge succeeds in transmitting power. In the WEOS scenario, for all p, the optimal resource placement is at the final layer, where each customer is given an individual, distributed resource. In the SEOS scenario ($m = 1$), when $p = 0.10$ and $p = 0.50$, the optimal resource placement is at the final layer. In the SEOS scenario for $p = 0.80$ (**Figure 3c**) and $p = 0.90$ (**Figure 3d**), the objective function exhibits an interior maximum in between layers 3 and 4 (for $p = 0.80$) and 2 and 3 (for $p = 0.90$), with optimal integer solutions at layer 4 and layer 3, respectively. When $p = 0.95$, the optimal resource placement in the SEOS scenario is at layer 2, as shown in **Figure 3e**. When $p = 0.99$, placing a single large resource at the root node maximizes the expected net benefit in SEOS scenario (**Figure 3f**).

To conclude, we see that a completely distributed architecture is optimal in the WEOS scenario for all instances of line reliability (p). In the SEOS scenario, a completely centralized architecture is optimal when power lines are extremely reliable ($p = 0.99$), resources are placed in intermediate layers when reliability (p) is between 0.80 and 0.95, and investing in customer-sited distributed resources is optimal when line reliability is $p = 0.50$ or lower.

4. Resilience analysis for a rectangular lattice topology

In the binary tree topology, there is an obvious choice for which nodes should be customer nodes, whereas in the rectangular lattice topology, which nodes should be considered “leaves” is not so obvious. We make the assumption that the boundary nodes of the lattice are customers, as shown in **Figure 4** where customer nodes are marked in orange. Similar to the binary tree analysis, our initial goal is to determine the probability that a customer located at each boundary node will

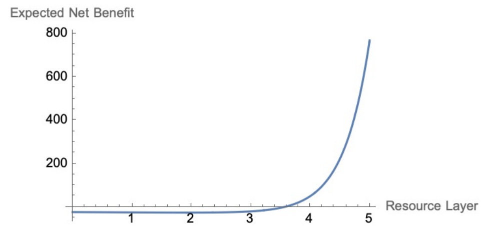

(a) $p = 0.10$

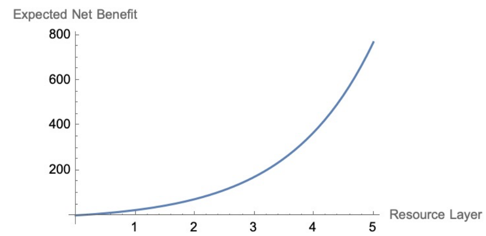

(b) $p = 0.50$

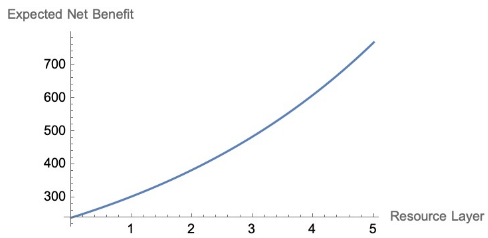

(c) $p = 0.80$

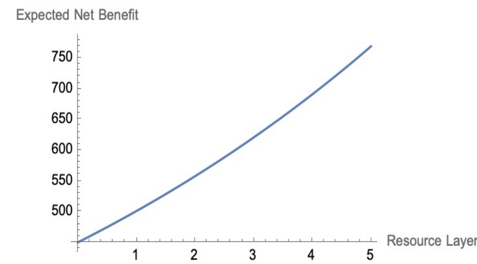

(d) $p = 0.90$

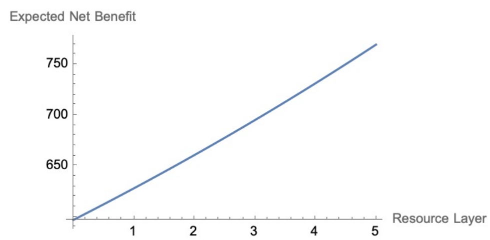

(e) $p = 0.95$

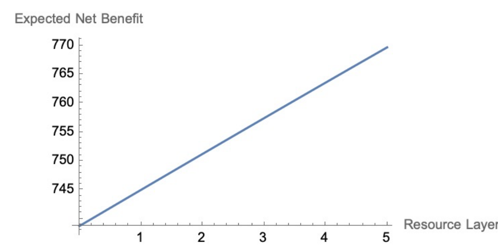

(f) $p = 0.99$

Figure 2. Expected net benefit as a function of the resource layer with weaker economies of scale ($h = 5,\ A = 20,\ C = 2,\ B = 25,\ m = 0.1$)

remain connected to a resource (i.e., continue to have electricity) after a disaster, given alternative resource placements. In the binary tree, the alternative resource placements were the layers in the tree. In this analysis of a rectangular lattice, we focus on a 17×17 lattice, since this lattice size allows us to consider various "regular" placements of resources within the grid and generally makes our analysis as analogous as possible to that of the binary tree.

4.1. Expected number of customers with power in a rectangular lattice

In the 17×17 lattice, if a single large resource is placed in the center of the grid (represented by the green box in **Figure 4**), then the lattice can be divided into four identical 9×9 quadrants (with some overlap, as we will address below). If resources are placed in the center of each 9×9 quadrant (represented by the yellow boxes in **Figure 4**), then each quadrant can be subdivided

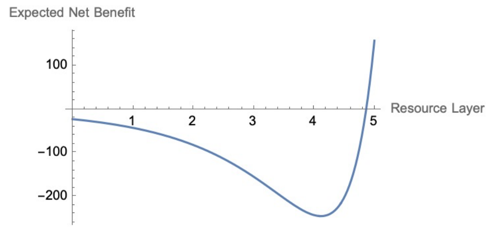

(a) $p = 0.10$

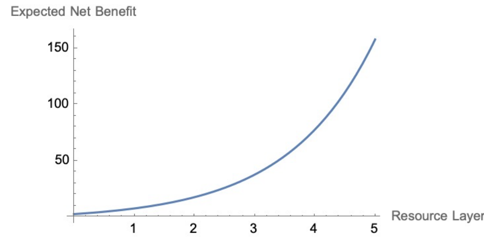

(b) $p = 0.50$

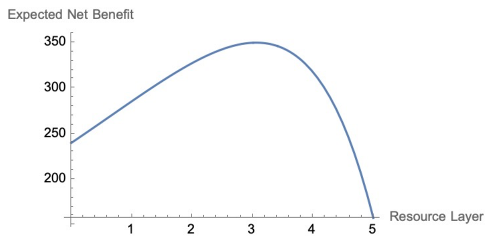

(c) $p = 0.80$

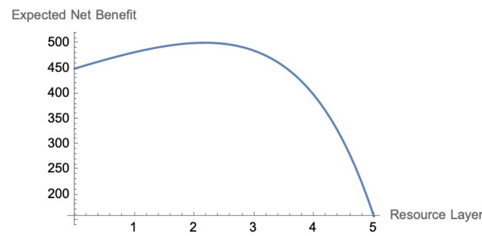

(d) $p = 0.90$

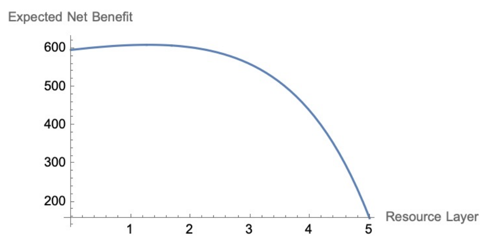

(e) $p = 0.95$

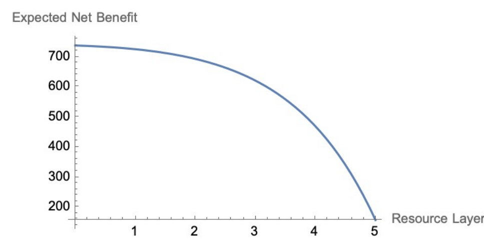

(f) $p = 0.99$

Figure 3. Expected net benefit as a function of the resource layer with stronger economies of scale ($h = 5,\ A = 20,\ C = 2,\ B = 25,\ m = 1$)

into four 5×5 quadrants. Furthermore, if resources are placed in the center of each 5×5 quadrant (represented by the blue boxes in **Figure 4**), then each quadrant can be subdivided into four 3×3 quadrants. Note that only 12 blue boxes appear in **Figure 4**, rather than the 16 that would be required to evenly cover the whole 17×17 lattice. This is because the customers only exist at the boundary nodes of the 17×17 lattice and they can thus be served by the 12 resources depicted in blue; we do not include resources in the interior of the grid as they are not needed to serve the customers. Similarly, the next alternative resource placement is represented by the 28 magenta boxes in **Figure 4**, and the final, most distributed resource placement would be to invest in 64 resource units with one located at each customer node (the orange nodes in the figure).

We assume that power only flows "outward" from each resource toward the customers that it serves. For example, for the single green resource in **Figure 4** to serve customers in the upper

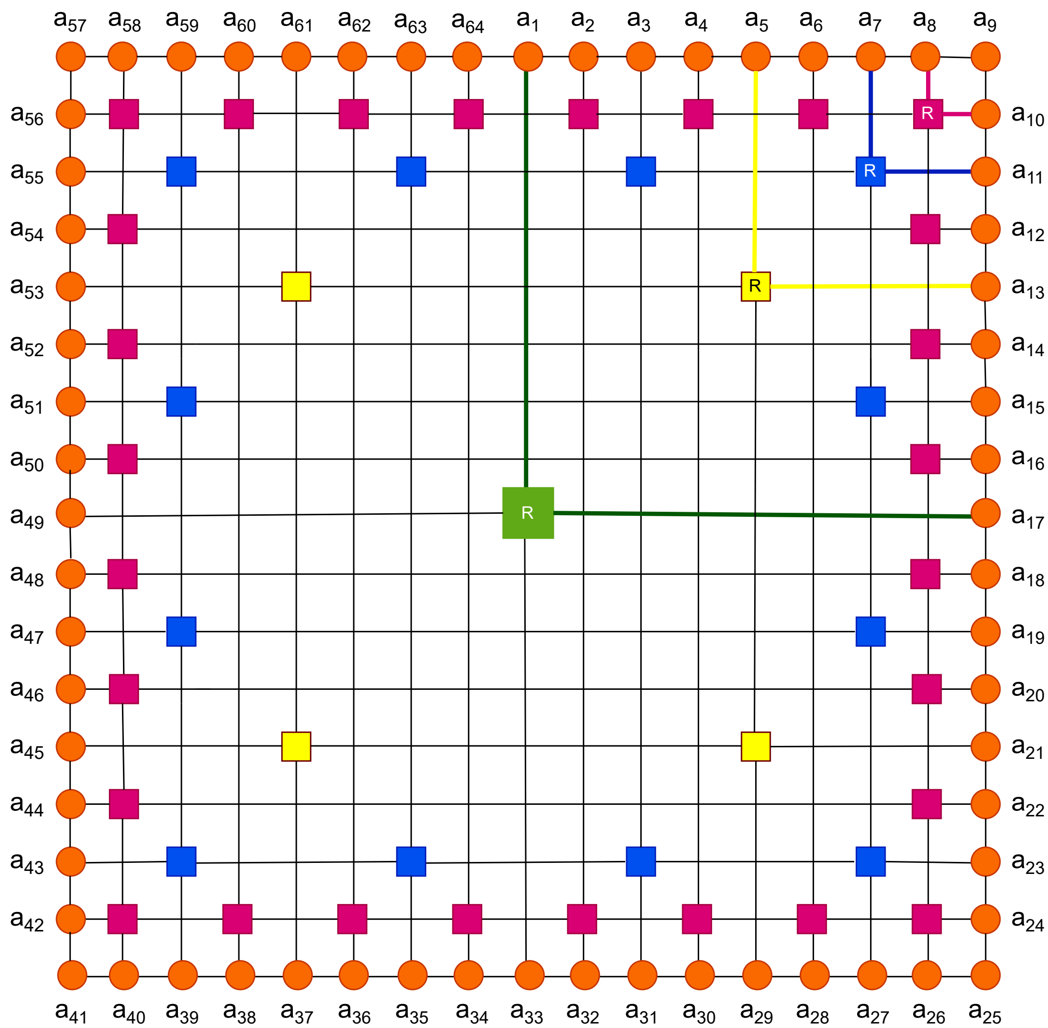

Figure 4. Rectangular lattice topology with four resource placement alternatives

right 9×9 quadrant of the lattice (i.e., customers at a_1 through a_{17}), power can only flow up or to the right. Our initial goal is to determine the probability that each customer will have power after a disaster, given the various possible resource placements. As before, we assume that each network edge is able to transmit power with probability p and that line failures are mutually independent. Unlike in the binary tree, where there was only one route from each resource to each customer, in the rectangular lattice there are often numerous routes connecting a resource to a customer. Due to the combinatorial nature of the lattice topology, deriving analytical expressions for the probabilities of having power is intractable. Therefore, we turn to numerical simulation to estimate these probabilities. It is important to note that if we estimate these probabilities for every node in one 9×9 quadrant (e.g., the upper right quadrant for the alternative with a single resource in the center), then we have all the estimates we need for all customer nodes and any resource placement. This is because the smaller quadrants associated with more distributed resource placements can be viewed as subsets of the largest (9×9) quadrant, and the probabilities of powering nodes are symmetric across the quadrants with a given resource placement.

Our Monte Carlo simulation of the 9×9 quadrant entails 50,000 samples, where each sample is generated by "flipping coins" to establish whether each power line remains operational (with probability p) or not (probability $1 - p$). Once a sample has been generated, we employ a depth-first search (DFS) algorithm to determine whether there is a viable path for power to flow from the resource to each node in the quadrant. By repeating this 50,000 times, we can divide the number of samples in which a node remains connected to a resource by 50,000 to obtain our estimate of the probability that this node will have access to electricity.

Figure 5 shows the results of our Monte Carlo simulation with $p = 0.90$ and the alternative resource placements that include 1, 4, 12, and 28 resources (in this order, from more centralized to more distributed). In **Figure 4**, these four resource placements are represented by the green, yellow, blue, and magenta boxes, respectively. In each subfigure of **Figure 5**, the probabilities of customers having power are the probabilities in the top row and right-most column (e.g., row 8 and column 8 in **Figure 5a**). We observe that the probabilities are lowest for the customers on the vertical and horizontal axes. For each of these customers, there is only a single path from the resource to the customer, so in order for them to have power, every line along the path must remain operational. In contrast, the probabilities are highest in the top right corner of each quadrant. Even though these customers are furthest away from the resource, this is more than offset by the greater number of paths connecting them to the resource. While power has to travel further to reach them, they benefit from the redundancy inherent in the rectangular lattice topology. Lastly, note that **Figure 5** demonstrates why we only needed to simulate the 9×9 quadrant. For example, the customer node in row 2 and column 0 of the 3×3 quadrant in **Figure 5c** is equivalent to the (non-customer) node in the same row and column of the 9×9 quadrant in **Figure 5a**.

Before moving on to analyze optimal resource placements in a rectangular lattice, it is helpful to briefly address the issue of overlap between quadrants. For example, consider the 1-resource placement (green box) and the customer located at node a_1 at the top of **Figure 4**. This node

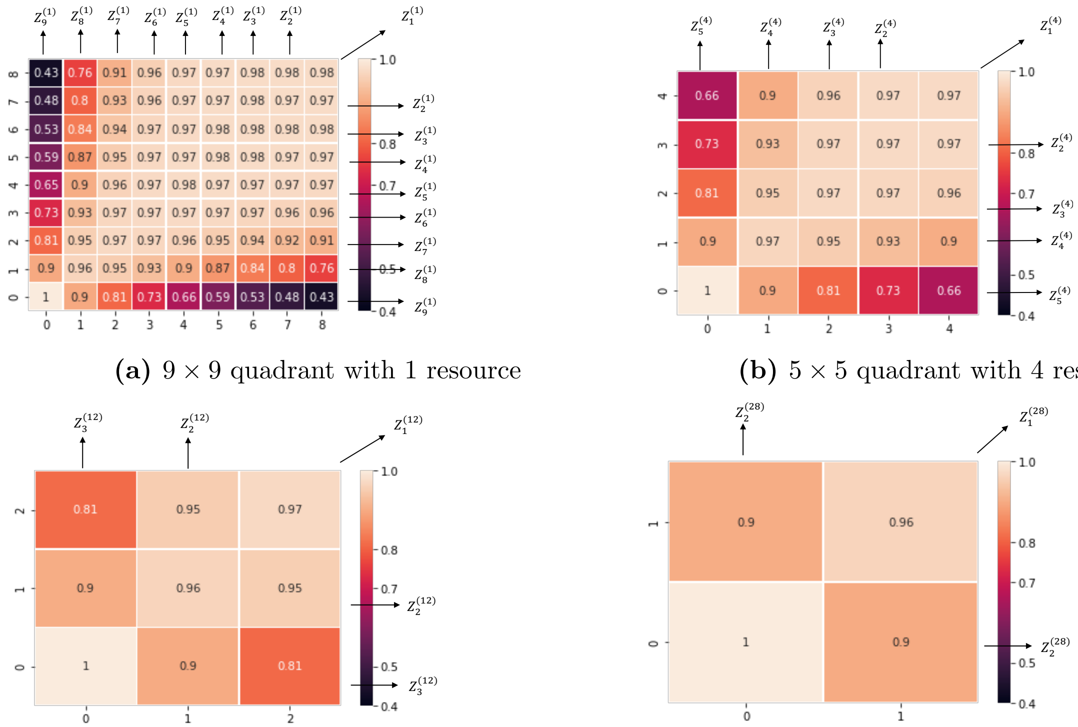

(a) 9×9 quadrant with 1 resource

(b) 5×5 quadrant with 4 resources

(c) 3×3 quadrant with 12 resources

(d) 2×2 quadrant with 28 resources

Figure 5. Simulated probabilities for alternative resource placements when $p = 0.90$

could be considered part of the upper right or upper left quadrant. In either case the probability that it will have power is the same, so we can arbitrarily assign it to one quadrant or the other. Next, consider the same node a_1 but with the 4-resource placement (yellow boxes). This node could be served by the resource located below it and to the left, or by the resource located below it and to the right. Again, regardless of which resource serves this customer, the probability of having power is the same. Therefore, we can arbitrarily assign it to one resource or the other. Importantly, note that we assume that each customer is only served by one resource. Therefore, whichever of the two resources the customer at a_1 is assigned to, it must remain connected to that specific resource in order to have access to electricity.

4.2. Optimal resource placement in a rectangular lattice

As in the binary tree analysis, the optimal resource placement in the rectangular lattice is the one that maximizes the expected net benefit, where benefits are associated with customers that have access to power and costs are associated with deploying resources in the grid. Whereas we approached the binary tree problem by solving a continuous optimization problem (and then using the optimal continuous solution to establish an optimal integer solution), for the rectangular lattice we establish expressions for the expected net benefit resulting from each possible resource placement. The notation used in these expressions is summarized in **Table 2**. For the probabilities written as $Z_i^{(k)}$, the superscript (k) refers to the resource placement (with k resources) and the subscript i refers to the customer node (see **Figure 5** for how these are numbered). There are five alternative resource placements – those with 1, 4, 12, 28, and 64 resources – and their expected net benefits are respectively:

1 resource:

$$4B\left(Z_1^{(1)} + 2\sum_{i=2}^{8} Z_i^{(1)} + Z_9^{(1)}\right) - d\left(A\left(\frac{d}{1}\right)^{-m} + C\right) \tag{8}$$

4 resources:

$$4B\left(2Z_1^{(4)} + 4\sum_{i=2}^{4} Z_i^{(4)} + 2Z_5^{(4)}\right) - d\left(A\left(\frac{d}{4}\right)^{-m} + C\right) \tag{9}$$

12 resources:

$$4B\left(4Z_1^{(12)} + 8Z_2^{(12)} + 4Z_3^{(12)}\right) - d\left(A\left(\frac{d}{12}\right)^{-m} + C\right) \tag{10}$$

28 resources:

$$8B\left(4Z_1^{(28)} + 4Z_2^{(28)}\right) - d\left(A\left(\frac{d}{28}\right)^{-m} + C\right) \tag{11}$$

64 resources:

$$64B - d\left(A\left(\frac{d}{64}\right)^{-m} + C\right). \tag{12}$$

Table 2. Notation for the rectangular lattice analysis

Variables	
Z	Experimental probabilities of customer nodes having power
Parameters	
p	Probability that an edge succeeds in power transfer
B	Monetary benefit per customer receiving power
d	Total power demand
A	Cost function scaling parameter
C	Theoretical lower bound on resource cost per unit capacity
m	A positive parameter that controls the strength of economies of scale

Each expression consists of two terms: the expected benefit of customers having power and the cost of resource placement. The cost term is based on the same cost function that we used for the binary tree analysis, which incorporates economies of scale controlled by the m parameter. The argument of the cost function for each resource placement is the total power demand d divided by the number of resources, which is the power capacity of each resource. To demonstrate how we constructed the expected benefit terms, consider the 1-resource placement in (8) and refer to its visualization in **Figure 5a**. Since the top row and right-most column are symmetric, this quadrant includes two customers whose probabilities of having power are $Z_i^{(1)}$ for each $i \in \{2, ..., 8\}$. This quadrant includes one customer whose probability is $Z_1^{(1)}$ and one whose probability is $Z_9^{(1)}$ (to avoid double counting customers in the overlaps, assign one of the corner customers to the next quadrant so that there are four total customers in the 17×17 lattice with probability $Z_9^{(1)}$). Finally, the expected benefit term is constructed by multiplying the sum of these customer probabilities along the quadrant boundary by 4 (because the quadrants are symmetric) and by B, the benefit of a customer having power.

4.3. Numerical analysis of a rectangular lattice

For the rectangular lattice, we consider two scenarios and numerically determine the optimal resource placement in each one by evaluating the expressions for the expected net benefits in (8)-(12). The two scenarios assume different values for the economies of scale parameter m. The first scenario features WEOS in resource investment ($m = 0.1$), while the second scenario features SEOS ($m = 1$). Within each scenario, we explore how the expected net benefit of each alternative resource placement varies with the probability of line success in transmitting power p. In both scenarios, we assume that each customer has an identical fraction of the total unit demand ($d = 1$), the monetary benefit per customer receiving power is $B = 25$, the cost function scaling parameter is $A = 20$, and the theoretical lower bound on cost per unit resource capacity is $C = 2$. Results from these scenarios are shown in **Figure 6**.

In the WEOS scenario with $m = 0.1$ (**Figure 6a**), for $p = 0.90$ and below, the 64-resource (most distributed) placement is optimal. However, when the probability of line success in power transfer is $p = 1$, the 1-resource (most centralized) placement is the optimal solution. In the SEOS scenario with $m = 1$ (**Figure 6b**), for $p = 0.50$ and below, the 64-resource (most distributed) placement is the optimal solution. In this setting for m, the 12-resource placement is the optimal solution when p is between 0.50 and 0.70, while the 1-resource (most centralized) placement is optimal when $p \geq 0.80$.

When the electric grid has perfect reliability in the rectangular lattice topology, the 1-resource (most centralized) placement is always the optimal solution. When $p \leq 0.5$, for the SEOS scenario, the 64-resource (most distributed) placement is the preferred alternative.

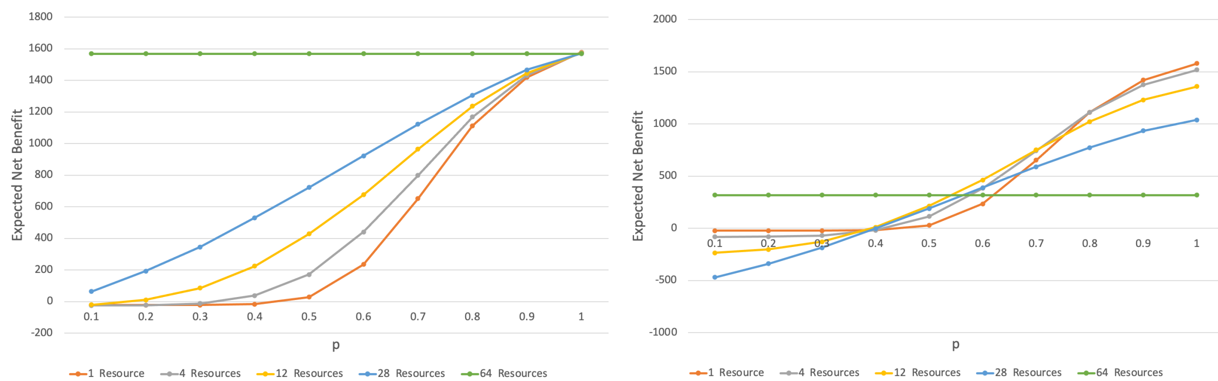

(a) $m = 0.1$ **(b)** $m = 1$

Figure 6. Expected net benefit when $B = 25$, $A = 20$, $C = 2$ and for different m

5. Comparison of binary tree and rectangular lattice

After analyzing the binary tree and rectangular lattice individually, in this section, we compare them to examine how the type of grid topology affects the choice between more centralized and more distributed resource placements. In the 17×17 rectangular lattice, irrespective of the resource placement, there are 64 customers located at the boundary nodes of the lattice. There are five alternative resource placements – those with 1, 4, 12, 28, and 64 resources. The binary tree that is most closely analogous to the 17×17 lattice is the tree with height $h = 6$, as it also features 64 customers located at the leaf nodes. One difference is that this binary tree offers seven resource placement alternatives with 1, 2, 4, 8, 16, 32, and 64 resources (the number of nodes in each layer). Nevertheless, since the 17×17 rectangular lattice and the binary tree with height $h = 6$ both serve 64 customers, we can compare their optimal resource placements to elucidate how the grid topology influences this decision.

To perform this comparison, we numerically analyze both topologies under two scenarios: WEOS and SEOS. In both scenarios, we set $B = 25$, $A = 20$, and $C = 2$. For both scenarios, we consider three different values for the probability that each line is able to transmit power: medium ($p = 0.6$), high ($p = 0.9$), and perfect reliability ($p = 1$). The WEOS and SEOS scenarios are distinguished by their values of the economies of scale parameter m, with $m = 0.1$ in the WEOS scenario and $m = 1$ in the SEOS scenario. Results for the two scenarios are presented in **Figure 7** and **Figure 8**, respectively. To plot the binary tree and lattice results on the same axes, the horizontal axes represent the number of resources in a placement.

In the WEOS scenarios with medium p (**Figure 7a**) and high p (**Figure 7b**), the 64-resource (most distributed) placements are the optimal solutions for both topologies. When $p = 1$ and the grid is perfectly reliable (**Figure 7c**), the 1-resource placements are the best alternatives for both the binary tree and rectangular lattice topologies, as expected.

In the SEOS scenario with medium p (**Figure 8a**), the 12-resource placement is the optimal solution for the rectangular lattice topology. However, for the binary tree topology, the optimal solution features either 32 or 64 resources, as these placements yield the same expected net benefit. The relationship between the number of resources deployed and the expected net benefit is completely different depending on whether the grid has a rectangular lattice or binary tree topology. In the SEOS scenario with high $p = 0.90$ (**Figure 8b**), the 1-resource placement is the optimal solution for the lattice topology. However, for the binary tree, the 8-resource placement is optimal. Once again, whenever the grid is perfectly reliable ($p = 1.0$) (**Figure 8c**), the 1-resource (most centralized) placements are optimal, as expected.

Examining the results presented in **Figure 7** and **Figure 8** in their totality, we see that centralized resource placements are more commonly optimal for a rectangular lattice topology while distributed resource placements are more commonly optimal for a binary tree topology. This finding can be explained by the greater path redundancy present in a rectangular lattice, whereas the binary tree only features a single path from each resource to each customer node. The lattice's greater redundancy makes power line failures less detrimental, which favors placing fewer (but larger) resources in more central grid locations to exploit economies of scale and reduce resource costs.

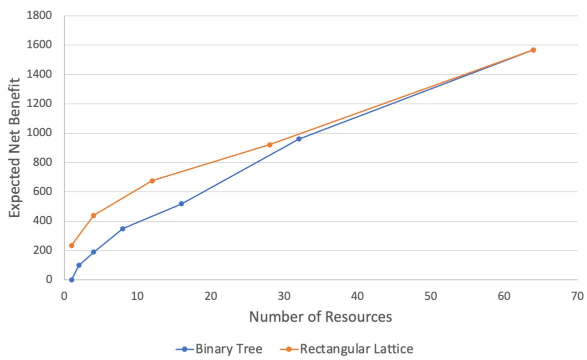

(a) $B = 25, A = 20, C = 2, m = 0.1, p = 0.60$

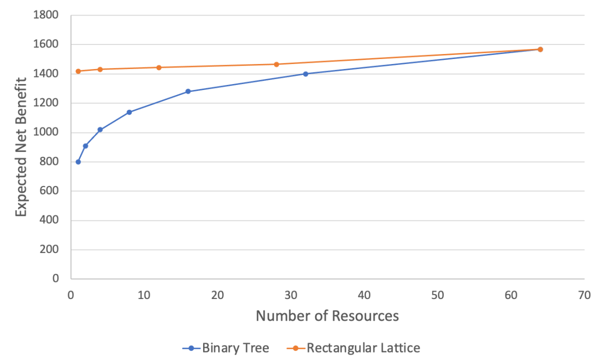

(b) $B = 25, A = 20, C = 2, m = 0.1, p = 0.90$

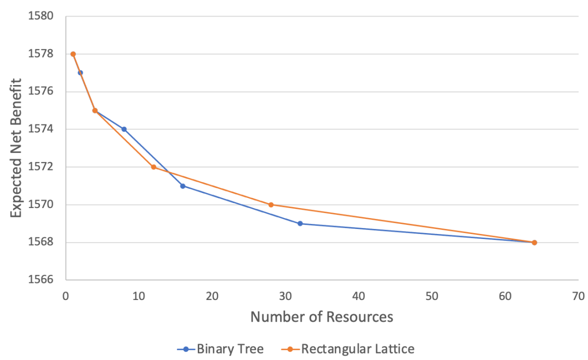

(c) $B = 25, A = 20, C = 2, m = 0.1, p = 1$

Figure 7. Expected net benefit for binary tree and rectangular lattice topologies with different p: weak economies of scale (WEOS) scenario

6. Conclusions

In this paper, we investigated the resilience of alternative electric grid configurations by adopting a stylized approach based on graph theory, probabilistic analysis, and simulation. We focused on the cost-benefit problem of optimally locating resources (e.g., generators, batteries) within electric grids where power line failures occur probabilistically. We designed the model to explore the tradeoff between resilience and cost considerations, where deploying a greater number of smaller resources closer to customers (i.e., pursuing a distributed resilience strategy) enhances resilience but increases cost due to economies of scale that make smaller resources more expensive per unit capacity. We considered the optimal resource placement problem for two types of grid topology: binary trees and rectangular lattices. For a binary tree, we derived the optimal resource placement analytically through a series of theoretical results, while for the rectangular lattice, we studied the problem numerically with probabilities estimated via simulation experiments. Lastly, we compared

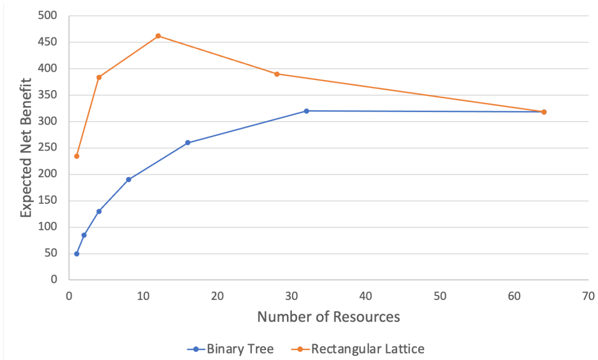

(a) $B = 25, A = 20, C = 2, m = 1, p = 0.60$

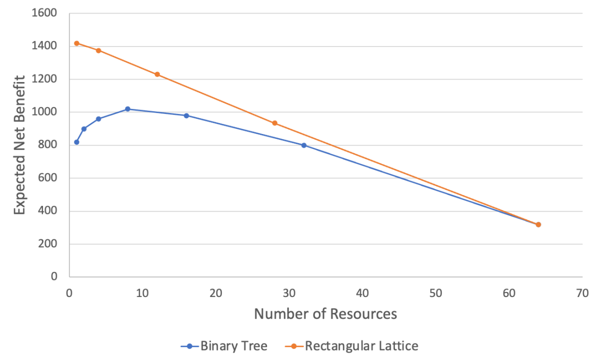

(b) $B = 25, A = 20, C = 2, m = 1, p = 0.90$

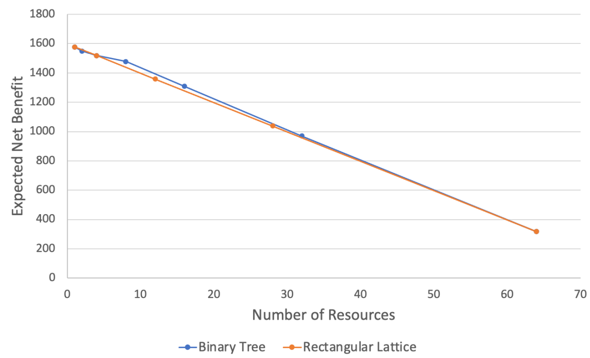

(c) $B = 25, A = 20, C = 2, m = 1, p = 1$

Figure 8. Expected net benefit for binary tree and rectangular lattice topologies with different p: strong economies of scale (SEOS) scenario

numerical results for a lattice and tree with the same number of customers to examine how the form of the network topology influences the optimal resource placement decision.

The preceding sections presented a number of detailed analytical and numerical results, and here we conclude by summarizing the most interesting high-level insights that our analysis revealed. Most importantly, we observed that the topology of the electric grid (in our case, whether it is a binary tree or a rectangular lattice) exerts a strong influence on whether centralized or distributed resource deployments maximize net benefits. While the optimal resource placement is sensitive to the parameters of a specific application, binary trees tend to favor more distributed placements where resources are closer to customers while rectangular lattices tend to favor more centralized placements where customers are served by fewer, but larger, resources. This key difference between the two topologies should be viewed as a consequence of their vastly different degrees of redundancy. In a binary tree there is one unique path from each resource to each customer, so as the path length increases, electricity access becomes more vulnerable to power line failures. Placing resources closer to customers is a natural strategy for circumventing the vulnerability of the grid. In contrast, in a rectangular lattice there are often many paths from resources to customers. The failure of any particular power line is less threatening in this setting with greater path redundancy, so centralized resource placements that reduce cost due to economies of scale are more likely to be optimal. For binary tree networks specifically, our theoretical results identified the interesting possibility that a decrease in power line reliability does not necessarily lead to an optimal resource placement that is closer to the customers. The logic is that a decrease in our p parameter also reduces the magnitude of the expected benefit term in the objective relative to the cost term, and cost becoming relatively more important pushes the optimal solution toward a more centralized placement that leverages economies of scale.

All of our results should be interpreted in light of the limitations of our stylized modeling approach, which does not attempt to represent real-world electric grids in a detailed manner. In the real world, most electric grids are not perfectly regular binary trees and rectangular lattices like the topologies that we studied in this paper. While we assumed that power line failures occur independently from each other, in reality, they are likely spatially dependent in that an extreme weather event would affect certain parts of the grid more than others. We considered as having access to power any customer who remained connected to a resource. This approach neglects capacity constraints of resources and lines that could limit the numbers of customers that they serve even if they remain connected. While these limitations are important to keep in mind, they were necessary to enable our more theoretical and general style of analysis, which we view as a valuable complement to the many computational studies of grid resilience in the existing literature.

This study suggests several promising directions for future research. Researchers could investigate the possibility of an analytical solution to the optimal resource placement problem on a rectangular lattice, which we explored numerically. It would also be valuable to extend our analysis to other network topologies that arise in real-world electric grids, beyond binary trees and rectangular lattices. In addition, future research could employ more detailed, computational power system models to test whether the insights we have derived on centralized versus distributed resource deployment hold in these more realistic grid representations.

7. ACKNOWLEDGMENTS

For this study, the authors received funding from the Energy Institute at The University of Texas at Austin.

References

Alderson, D. L., Brown, G. G., and Carlyle, W. M. (2015). Operational models of infrastructure resilience. *Risk Analysis*, 35(4):562–586.

Aros-Vera, F., Gillian, S., Rehmar, A., and Rehmar, L. (2021). Increasing the resilience of critical infrastructure networks through the strategic location of microgrids: A case study of Hurricane Maria in Puerto Rico. *International Journal of Disaster Risk Reduction*, 55:102055.

Ashrafi, R., Amirahmadi, M., Tolou-Askari, M., and Ghods, V. (2021). Multi-objective resilience enhancement program in smart grids during extreme weather conditions. *International Journal of Electrical Power & Energy Systems*, 129:106824.

Bessani, M., Massignan, J. A. D., Fanucchi, R. Z., Camillo, M. H. M., London, J. B. A., Delbem, A. C. B., and Maciel, C. D. (2019). Probabilistic assessment of power distribution systems resilience under extreme weather. *IEEE Systems Journal*, 13(2):1747–1756.

Brown, M. A. and Soni, A. (2019). Expert perceptions of enhancing grid resilience with electric vehicles in the United States. *Energy Research & Social Science*, 57:101241.

Busby, J. W., Baker, K., Bazilian, M. D., Gilbert, A. Q., Grubert, E., Rai, V., Rhodes, J. D., Shidore, S., Smith, C. A., and Webber, M. E. (2021). Cascading risks: Understanding the 2021 winter blackout in Texas. *Energy Research & Social Science*, 77:102106.

Chang, S. E., McDaniels, T., Fox, J., Dhariwal, R., and Longstaff, H. (2014). Toward disaster-resilient cities: Characterizing resilience of infrastructure systems with expert judgments. *Risk Analysis*, 34(3):416–434.

Chen, X., Qiu, J., Reedman, L., and Dong, Z. Y. (2019). A statistical risk assessment framework for distribution network resilience. *IEEE Transactions on Power Systems*, 34(6):4773–4783.

Curt, C. and Tacnet, J.-M. (2018). Resilience of critical infrastructures: Review and analysis of current approaches. *Risk Analysis*, 38(11):2441–2458.

Forssén, K. and Mäki, K. (2016). Resilience of Finnish electricity distribution networks against extreme weather conditions. In *CIRED Workshop 2016*, pages 1–4. IET.

Gallaher, A., Graziano, M., and Fiaschetti, M. (2021). Legacy and shockwaves: A spatial analysis of strengthening resilience of the power grid in Connecticut. *Energy Policy*, 159:112582.

Galvan, E., Mandal, P., and Sang, Y. (2020). Networked microgrids with roof-top solar PV and battery energy storage to improve distribution grids resilience to natural disasters. *International Journal of Electrical Power & Energy Systems*, 123:106239.

Gharehveran, S. S., Ghassemzadeh, S., and Rostami, N. (2022). Two-stage resilience-constrained planning of coupled multi-energy microgrids in the presence of battery energy storages. *Sustainable Cities and Society*, 83:103952.

Ishiwata, H. and Yokomatsu, M. (2018). Dynamic stochastic macroeconomic model of disaster risk reduction investment in developing countries. *Risk Analysis*, 38(11):2424–2440.

Kemabonta, T. (2021). Grid Resilience analysis and planning of electric power systems: The case of the 2021 Texas electricity crises caused by winter storm Uri (# TexasFreeze). *The Electricity Journal*, 34(10):107044.

Kizito, R., Li, X., Sun, K., and Li, S. (2020). Optimal distributed generator placement in utility-based microgrids during a large-scale grid disturbance. *IEEE Access*, 8:21333–21344.

LaCommare, K. H., Eto, J. H., Dunn, L. N., and Sohn, M. D. (2018). Improving the estimated cost of sustained power interruptions to electricity customers. *Energy*, 153:1038–1047.

Laws, N. D., Anderson, K., Diorio, N. A., Li, X., and McLaren, J. (2018). Impacts of valuing resilience on cost-optimal PV and storage systems for commercial buildings. *Renewable Energy*, 127:896–909.

Liu, J., Jian, L., Wang, W., Qiu, Z., Zhang, J., and Dastbaz, P. (2021). The role of energy storage systems in resilience enhancement of health care centers with critical loads. *Journal of Energy Storage*, 33:102086.

Liu, X., Shahidehpour, M., Li, Z., Liu, X., Cao, Y., and Bie, Z. (2016). Microgrids for enhancing the power grid resilience in extreme conditions. *IEEE Transactions on Smart Grid*, 8(2):589–597.

Ma, S., Chen, B., and Wang, Z. (2016). Resilience enhancement strategy for distribution systems under extreme weather events. *IEEE Transactions on Smart Grid*, 9(2):1442–1451.

Ma, S., Su, L., Wang, Z., Qiu, F., and Guo, G. (2018). Resilience enhancement of distribution grids against extreme weather events. *IEEE Transactions on Power Systems*, 33(5):4842–4853.

Masrur, H., Sharifi, A., Islam, M. R., Hossain, M. A., and Senjyu, T. (2021). Optimal and economic operation of microgrids to leverage resilience benefits during grid outages. *International Journal of Electrical Power & Energy Systems*, 132:107137.

Mishra, S. and Anderson, K. (2021). Probabilistic resilience of DER systems - a simulation assisted optimization approach. In *2021 IEEE Power Energy Society Innovative Smart Grid Technologies Conference (ISGT)*, pages 1–5.

Najarian, M. and Lim, G. J. (2019). Design and assessment methodology for system resilience metrics. *Risk Analysis*, 39(9):1885–1898.

Panteli, M. and Mancarella, P. (2015). The grid: Stronger, bigger, smarter?: Presenting a conceptual framework of power system resilience. *IEEE Power and Energy Magazine*, 13(3):58–66.

Poudel, S., Dubey, A., and Bose, A. (2019). Probabilistic quantification of power distribution system operational resilience. In *2019 IEEE Power Energy Society General Meeting (PESGM)*, pages 1–5.

Sepúlveda-Mora, S. B. and Hegedus, S. (2022). Resilience analysis of renewable microgrids for commercial buildings with different usage patterns and weather conditions. *Renewable Energy*, 192:731–744.

Sharma, P. and Chen, Z. (2020). Probabilistic resilience measurement for rural electric distribution system affected by hurricane events. *ASCE-ASME Journal of Risk and Uncertainty in Engineering Systems, Part A: Civil Engineering*, 6(2):04020021.

Siskos, E. and Burgherr, P. (2022). Multicriteria decision support for the evaluation of electricity supply resilience: Exploration of interacting criteria. *European Journal of Operational Research*, 298(2):611–626.

Trakas, D. N., Panteli, M., Hatziargyriou, N. D., and Mancarella, P. (2019). Spatial risk analysis of power systems resilience during extreme events. *Risk Analysis*, 39(1):195–211.

Watson, E. B. and Etemadi, A. H. (2020). Modeling Electrical Grid Resilience Under Hurricane Wind Conditions With Increased Solar and Wind Power Generation. *IEEE Transactions on Power Systems*, 35(2):929–937.

Wender, B. A., Morgan, M. G., and Holmes, K. J. (2017). Enhancing the Resilience of Electricity Systems. *Engineering*, 3(5):580–582.

Zamuda, C. D. and Ressler, A. (2020). Federal adaptation and mitigation programs supporting Community investment in electricity resilience to extreme weather. *The Electricity Journal*, 33(8):106825.

Zhang, X., Tu, H., Guo, J., Ma, S., Li, Z., Xia, Y., and Tse, C. K. (2021). Braess paradox and double-loop optimization method to enhance power grid resilience. *Reliability Engineering & System Safety*, 215:107913.